34th Annual International Conference of the IEEE EMBS
San Diego, California USA, 28 August - 1 September, 2012

# Point-Guided Modeling and Segmentation of Myocardium for Low Dose Cardiac CT Images

Yixun Liu, Marcelo Souto Nacif, Songtao Liu, Christopher T. Sibley,
David A. Bluemke, Ronald M. Summers, and Jianhua Yao

***Abstract*— Cardiac CT is emerging as a preferable modality to detect myocardial stress/rest perfusion; however the insufficient contrast of myocardium on CT image makes its segmentation difficult. In this paper, we present a point-guided modeling and deformable model-based segmentation method. This method first builds a triangular surface model of myocardium through Bézier contour fitting based on a few points selected by clinicians. Then, a deformable model-based segmentation method is developed to refine the segmentation result. The experiments on 8 cases show the accuracy of the segmentation in terms of true positive volume fraction, false positive volume fractions, and average surface distance can reach 91.0%, 0.3%, and 0.6mm, respectively. The comparison between the proposed method and a graph cut-based method is performed. The results demonstrate that this method is effective in improving the accuracy further.**

## I. Introduction

Myocardium extracellular volume fraction (ECV) is highly associated with diffuse myocardial fibrosis, a hallmark of pathologic remodeling. Compared to cardiac MRI, low dose cardiac CT provides a fast way to assess ECV; however the insufficient contrast of myocardium on CT image makes the myocardium segmentation the main barrier for its clinical use.

Ecabert et al. presented a model-based approach for the whole heart segmentation [1]. First, pose misalignment is corrected by matching the model to the image using a global similarity transformation, and then the model is deformed to match the boundaries of the patient's anatomy. In [2], Jolly provided a method to automatically extract the myocardium by first a global localization of the left ventricle and then a region based Expectation and Maximization segmentation. Chen et al. presented a hybrid method by integrating the shape prior information with the graph cut (GC) method [3]. A pseudo-3D strategy is applied for the initialization based on the live wire (LW) method, and then the shape information generated from the initialization step is integrated into a GC cost function.

Shape constrains is valuable in improving the accuracy of the segmentation, especially in the region where no strong edges exist; however due to the large variation of the myocardial shape, aligning an established shape with the object is not a robust approach, which motivates us to develop a patient specific myocardial model based on sparse point set. Unlike the modeling method provided in [4], where an initial regular Ellipsoid is fitted to the 3D guided-points by minimizing an error function consisting of the sum of a smoothing term and a point matching term, we present a Bézier contour [5,6] based modeling method. This method does not need to deform an initial model, therefore avoiding the deterioration of the element quality. The proposed method needs some points selected in the short axis slices in order to automatically build contours and construct surface from the contours.

Along with this model, a deformable model-based segmentation method is developed. This method incorporates region information and shape constraints into one energy function. The initial model, provided by the proposed modeling method, will be driven by the energy function to match the myocardial boundary.

Yixun Liu, Marcelo Souto Nacif, Songtao Liu, Chris Sibley, David A. Bluemke, Ronald M. Summers, and Jianhua Yao are with the Radiology and Imaging Science, National Institutes of Health. (yixun.liu@nih.gov, JYao@cc.nih.gov).

## II. Method

### A. Point-guided myocardium modeling

Using a few points selected by clinicians to create a patient specific model is helpful in providing an initial estimation and imposing shape constraints for model-based segmentation.

The basic idea to build the myocardium model is to use clinician specified points to create interlaced Bézier contours along both longitude and latitude directions. The intersection points of these Bézier contours are first connected to constitute quadrilateral and triangular elements, and then each quadrilateral element is further divided into two triangles to produce a triangular mesh. This procedure is performed on both endocardium (endo) and epicardium (epi) to produce endo and epi surface models, and then these two meshes are combined into one closed myocardial surface model. Fig. 1 shows the flowchart of this method, in which the left side and the right side create the endo surface and the epi surface, respectively.

1) Both endo and epi surface meshes begin from a few points selected by a clinician. In addition to the apex, the other points are selected in the basal, middle, and apical short axis slices as suggested by American Heart Association (AHA) in standard myocardial segmentation [7].There is no stringent requirement for selecting the points within the slice. Roughly evenly spaced four points are acceptable as shown in the left image of Fig.2 if we do not consider the segmentation of papillary muscles.

2) Next, a Bézier curve is fitted on each of the basal, middle and apical slices as shown in the right image of Fig. 2 (along with one apex point), for the following automatic myocardial modeling.

 

3) Produce longitude Bézier contours. Each contour is resampled along the longitude direction. The number of reampled points is determined by the parameter: *longitude resolution*. These resampled points are used to produce longitude Bézier contours intersected at the apex as shown in the left image of Fig. 3.

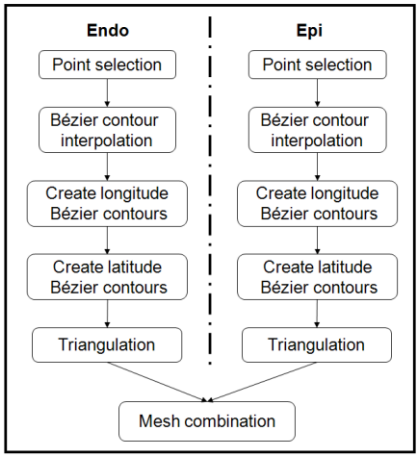


Figure 1. Flowchart of myocardial modeling. Left: endo modeling. Right: epi modeling.

4) The longitude Bézier contours are resampled along the latitude direction with specified *latitude resolution*, and Bézier fitting is performed to produce latitude Bézier contours.

5) The intersection points of the interlaced Bézier contours are connected to produce quadrilateral elements if there is no apex in four neighboring points, otherwise producing triangular elements. For each quadrilateral element, it is further divided into two connected triangles, leading to a triangular surface mesh as shown in the right image of Fig. 3.

6) The above procedures are performed on both endo and epi to produce two triangular surface meshes as shown in the left image of Fig. 4. The vertices located in the basal planes of the two meshes are connected to produce the final closed myocardium surface model as shown in the right image of Fig. 4. The proposed modeling technique is robust and easy to be implemented because the basic operation involved in the modeling is Bézier curve fitting. The modeling approach uses Bézier curve fitting three times: Bézier contours in short axis slices, longitude and latitude Bézier contours. The resulting model will be used as the initial segmentation for the subsequent deformable model-based segmentation.

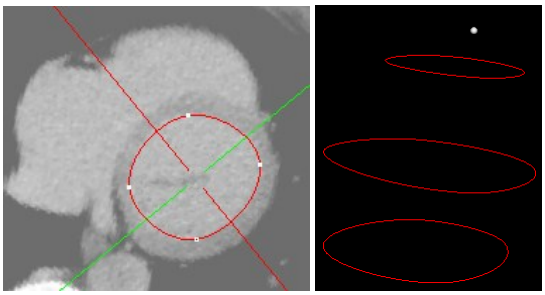

Figure 2. Left: Four endo points are selected in the basal short axis slice. Right: Bézier contours and the apex used for the endo modeling.

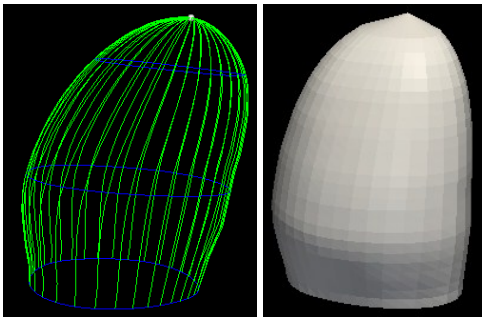

Figure 3. Left: Longitude Bézier contours. Right: Resulting endo model.

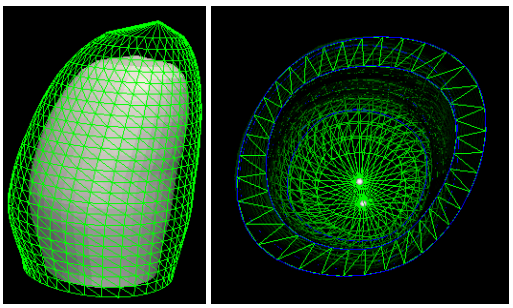

Figure 4. Left: endo and epi surfaces. Right: Myocardial model by connecting the endo and epi surfaces at the bottom.

### *B. Deformable model-based segmentation*

The myocardial model described above not only provides a good initial segmentation result, thus avoiding local minima, but also provides a shape constraint for the subsequent deformable model-based segmentation.

The myocardium in the low dose CT image does not demonstrate strong edges with surrounding tissues, but shows strong Gaussian distribution. We develop an energy function by exploring the region information and imposing shape constraints.

The energy function, which will drive the model evolution, is defined as,

$$E(u) = \lambda_1 \frac{1}{|\Omega_u|} \iiint_{\Omega_u} (I(x,y,z) - \bar{I})^2 d\Omega + \iint_{\partial\Omega_u} Lu(x,y,z) dS - \lambda_2 |\Omega_u| \quad (1)$$

where $u$ is the unknown deformation field. $\Omega_u$ is the region surrounded by surface $\partial\Omega_u$, which is the initial surface (Bézier model) deformed by $u$. $L$ is a smoothing operator. $\bar{I}$ is the mean intensity of image $I$ within $\Omega_u$. The first term measures the variation of the intensity in the region, the second term measures the smoothness of the deformation field, and the third term measures the volume of the region. When $E$ reaches the minimal, a region characterized by 1) grouping voxels with similar intensity, 2)

smoothly deviated from the initial model, and 3) including as many voxels as possible, will be found.

The variation of the intensity and the tightness of the cluster are controlled by $\lambda_1$ and $\lambda_2$, respectively. To effectively find the numeric solution, equation (1) is approximated by representing the unknown region $\Omega_u$ with the region, denoted by $R_{M_D}$, surrounded by a mesh $M_D$. The evolution of the mesh is restricted in the normal direction, i.e. for a vertex $v_i$, it only moves along its normal direction with a distance $d_i$. This approximation is able to maintain the mesh quality as evolving and significantly lower the pressure of optimizer since moving along the mesh surface does not contribute to minimizing the energy function, except increasing the pressure of optimizer. $D$ is the vector concatenated from $d_i$. $M_D$ denotes the mesh evolving from the initial mesh $M_0$, produced by Bézier modeling, with a distance vector $D$. Smoothing operator $L$, is approximated by the degree of the relative movement between the current vertex and its neighboring vertices. As a result, equation (1) is approximated by

$$E(D) = \lambda_1 \frac{1}{\left|R_{M_D}\right|} \sum_{i,j,k \in R_{M_D}} (I(i,j,k) - \bar{I})^2 + \sum_{v \in S_{M_D}} (d_v - \frac{1}{\left|N_v\right|} \sum_{s \in Nv} d_s)^2 - \lambda_2 \left|R_{M_D}\right| \quad (2)$$

where $S_{M_D}$ is the surface of mesh $M_D$, $N_v$ is the neighboring set of vertex $v$, and $\left|R_{M_D}\right|$ is the number of voxels within mesh $M_D$. $\left|R_{M_D}\right|$ can be calculated by voxelization, a rasterization technique. The equation (2) is solved by L-BFGS optimization, which is a gradient-based efficient method, especially suitable for high dimensional optimization problems [8].

## III. Results

The proposed method was evaluated on 8 clinical low dose CT datasets, acquired from post-contrast phases of a 320-MDCT scanner (Aquilion One, Toshiba Medical Systems, Tustin, CA). The slice thickness is 3 mm and in-plane pixel size is 0.37×0.37 mm. The image size is 512×512×47. We compare this method with GC segmentation developed in [3] and manually segmentation produced by an expert using our mesh edit tool.

Fig. 5 shows the mesh evolution in 3D (left figure) and 2D (right figure) spaces, from the initial green mesh, produced by our modeling method, to the final red mesh, produced by our deformable model-based segmentation.

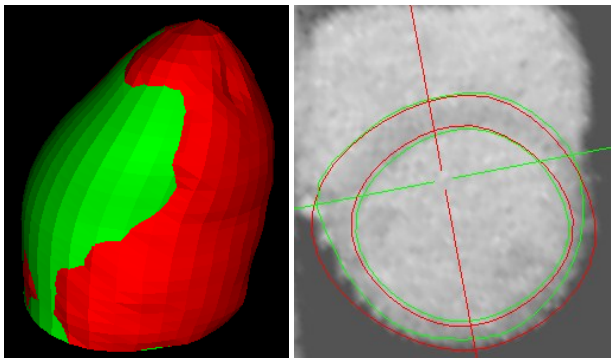

Figure 5. Evolved model and contours. Left: Initial model (green model) evolves to the final model (red model). Right: Initial contour evolves to the final contour in the short axis slice.

Fig. 6 shows the segmented myocardium in the long axis slice (left figure) and the short axis slice (right figure) for two different cases. The green contour is the reference result, produced by an expert by manually adjusting myocardial surface. The red contour comes from the automatic segmentation method.

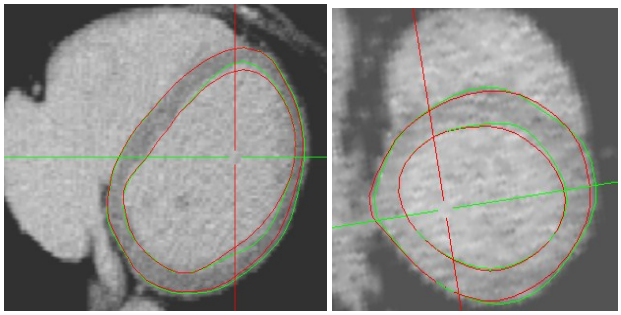

Figure 6. Deformable model segmentation results. Red contour is the result produced by the proposed method, and the green contour is the reference contour. Left: the CT image of a 45 years old female. Right: the CT image of a 61 years old female.

We compare our method with GC method and show the results in Fig. 7 and Fig. 8, respectively. The segmentation result is represented by a binary image and superimposed on the reference contour. Compared to the right figure (GC result), the result in the left figure (proposed method) is smoother and matches the boundary well.

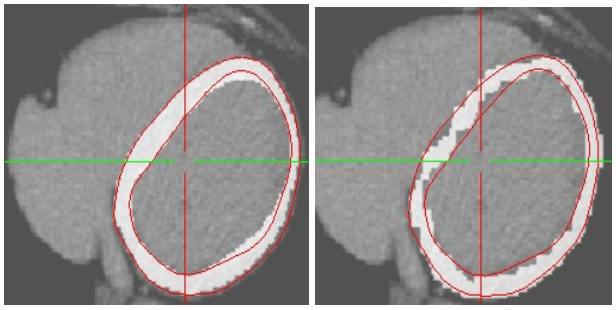

Figure 7. Comparison between the proposed method and the GC method in the long axis slice. Left: proposed method. Right: GC method. The binary image is the segmentation result, and the contour is the reference.

TABLE I. Quantitative evaluation on 8 cases. $\lambda_1$=1.0, $\lambda_2$=0.005, longitude resolution = 36, latitude resolution = 20. TPVF: true positive volume fractions, FPVF: false positive volume fractions, ASD: average surface distance. The values in the parenthesis are the results from GC method.

| | *1* | *2* | *3* | *4* | *5* | *6* | *7* | *8* | *mean±deviation* |
|---|---|---|---|---|---|---|---|---|---|
| TPVF (%) | 84.2 (53.9) | 94.2 (56.1) | 94.7 (65.0) | 97.4 (58.1) | 84.5 (65.5) | 90.6 (61.8) | 93.1 (69.9) | 89.3 (57.5) | 91.0±4.8 (61.0±5.5) |
| FPVF (%) | 0.4 (0.2) | 0.1 (0.5) | 0.2 (0.3) | 0.3 (0.3) | 0.4 (0.4) | 0.2 (0.5) | 0.2 (0.3) | 0.2 (0.2) | 0.3±0.1 (0.3±0.1) |
| ASD (mm) | 0.8 (0.5) | 0.4 (2.7) | 0.4 (0.7) | 0.7 (0.8) | 0.7 (0.7) | 0.3 (1.2) | 0.5 (0.6) | 0.6 (0.4) | 0.6±0.2 (1.0±0.7) |

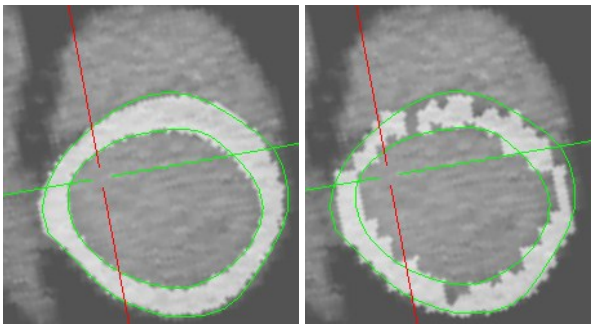

Figure 8. Comparison between the proposed method and the GC method in the short axis slice. Left: proposed method. Right: GC method. The binary image is the segmentation result, and the contour is the reference.

The results of the quantitative evaluation of the proposed approach are presented in Table I. The accuracy in terms of true positive and false positive volume fractions (TPVF and FPVF) [9], and average surface distance (ASD) is shown. TPVF indicates the fraction of the total amount of tissue in the true delineation, and FPVF denotes the amount of tissue falsely identified. They are defined as follows,

$$TPVF = \frac{\left|S_{seg} \cap S_{ref}\right|}{\left|S_{ref}\right|}, FPVF = \frac{\left|S_{seg} - S_{seg} \cap S_{ref}\right|}{\left|S_{whole} - S_{ref}\right|} \quad (3)$$

where $S_{seg}$ denotes the extracted voxel set in the segmented image, $S_{ref}$ denotes the extracted voxel set in the reference image, and $S_{whole}$ denotes the voxel set in the whole image. $|\cdot|$ is the cardinality measure of a set.

In Table I, the proposed method demonstrates much higher TPVF than GC method, but similar value regarding FPVF. This can be interpreted by a conservative segmentation in GC method.

## IV. Conclusion

In this paper, we present a Bézier curve based myocardial modeling method. With sparse points distributed in basal, middle, and apical slices, a closed triangular surface mesh can be generated. Based on this model, a deformable model based segmentation method is presented to refine the segmentation result. The advantage of the proposed method is the produced patient specific model is smooth and close to the real myocardial boundary, therefore effectively avoiding local minimal for the subsequent model-based segmentation.

The model-based segmentation explores the region information rather than the edge information, therefore effectively avoiding the influence of the noise. The experiments on 8 cases verify the effectiveness of this method, and the comparison with GC method shows the segmentation result of the proposed method is smoother and more accurate.

## Acknowledgment

This research was supported in part by the Intramural Research Program of the Clinical Center, NIH.

## References

[1] O. Ecabert, J. Peters, H. Schramm, C. Lorenz, J. Berg, M.J. Walker, M. Vembar, M.E. Olszewski, K. Subramanyan, G. Lavi, and J. Weese, "Automatic Model-Based Segmentation of the Heart in CT Images,", *IEEE* Transactions on *Medical Imaging*, vol.27, no.9, pp.1189-1201, Sept. 2008.

[2] Marie-Pierre Jolly, "Automatic Segmentation of the Left Ventricle in Cardiac MR and CT Images," Int. J. Comput. Vision vol.70, no.2, pp. 151-163, Nov. 2006.

[3] Xinjian Chen, Ronald M. Summers, Marcelo Souto Nacif, Songtao Liu, David A. Bluemke, and Jianhua Yao, "A framework of whole heart extracellular volume fraction estimation for low dose cardiac CT images," Proc. SPIE 8314, 831429, 2012.

[4] Alistair A. Young, Brett R. Cowan, Steven F. Thrupp, Warren J. Hedley, and Louis J. Dell'Italia, "Left Ventricular Mass and Volume: Fast Calculation with Guide-Point Modeling on MR Images," Radiology, vol. 216, pp. 597-602, Aug. 2000.

[5] Bartels, R. H.; Beatty, J. C.; and Barsky, B. A. "Bézier Curves," Ch. 10 in An Introduction to Splines for Use in Computer Graphics and Geometric Modelling. San Francisco, CA: Morgan Kaufmann, pp. 211-245, 1998.

[6] M. Dæhlen, T. Lyche, and L.L. Schumaker (eds.), "Convex surface fitting with parametric Bézier surfaces," Mathematical Methods for Curves and Surfaces II, Vanderbilt University Press, Nashville, pp. 263-270, 1998.

[7] American Heart Association, "Standardized Myocardial Segmentation and Nomenclature for Tomographic Imaging of the Heart," Circulation vol.105, no.4, pp. 539-542, 2002.

[8] J. Nocedal and S.J. Wright, "Numerical optimization," Springer Verlag, 1999.

[9] Udupa JK, Leblanc VR, Zhuge Y, Imielinska C, Schmidt H, Currie LM, Hirsch BE, and Woodburn J, "A framework for evaluating image segmentation algorithms," Computerized Medical Imaging and Graphics, vol.30, no.2, pp. 75-87, 2006.